



PHASE DIAGRAM OF QUASI-ONE-DIMENSIONAL METALS AND SUPERCONDUCTIVITY IN THE  $(\text{TMTSF})_2\text{X}$  COMPOUNDS

B. Horovitz

Department of Physics, The Weizmann Institute of Science, Rehovot, Israel

H. Gutfreund and M. Weger

Racah Institute of Physics, Hebrew University, Jerusalem, Israel

(Received 2 April, 1981 by S. Alexander)

**Abstract:** The phase diagram of a quasi-one-dimensional metal is derived for a system with interchain tunneling. Retarded and nonretarded forward and backward scattering interactions are included. We show that singly charged acceptor molecules produce a potential along the conducting chains which leads to a retarded umklapp scattering. This umklapp scattering depends strongly on the phonon frequency and can explain the crossover of spin density wave to superconductivity as function of pressure as observed in  $(\text{TMTSF})_2\text{X}$  compounds.

The recent interest in the instabilities of quasi-one-dimensional metals was enhanced by the discovery of the  $(\text{TMTSF})_2\text{X}$  ( $\text{X} = \text{PF}_6, \text{AsF}_6, \text{NO}_3, \text{ClO}_4, \dots$ ) "monochain" compounds in which only the donor chains of TMTSF molecules participate in the electron transport.<sup>1</sup> Five compounds in this family have already been shown to undergo a superconducting phase transition.  $(\text{TMTSF})_2\text{PF}_6$  has at ambient pressure a metal-insulator transition at 18°K and becomes superconducting above 12 Kbar below 0.9°K.<sup>2</sup> Both transition temperatures decrease with pressure. There is growing evidence that the insulating phase is a spin-density wave<sup>3,4</sup> (SDW) rather than a charge-density wave as in the other organic conductors. Similar behaviour is observed for  $\text{X} = \text{AsF}_6, \text{SbF}_6, \text{TaF}_6$ .<sup>5</sup> It was shown recently that the compound  $(\text{TMTSF})_2\text{ClO}_4$  exhibits superconductivity at ambient pressure.<sup>6</sup> The explanation of the rich phenomenology of these compounds imposes severe restrictions on possible theoretical phase diagrams. We shall show that the conventional phase-diagram of one-dimensional metals, based on forward and backward scattering only is unlikely to account for the observed behaviour.

The  $(\text{TMTSF})_2\text{X}$  class of compounds has several novel features of which, we believe, the most important for the understanding of the phase transitions is the special role of the singly charged acceptor molecules. The structure of the acceptor chains has a glide plane symmetry so that they do not couple directly to electrons moving along the donor chains. (The glide plane symmetry of the whole compound is only approximate because of the small tilt-angle of the donor molecules). Thus there is no gap in the electron spectrum in the middle of the band unless there is a transverse component in the electron motion. The potential from these chains has a periodicity of  $\frac{1}{2}4k_F$  where  $k_F$  is the Fermi wavevector of the  $\frac{1}{2}$  filled band on the TMTSF chain. If the glide plane symmetry

is absent, such a potential usually generates an umklapp scattering with the lowest order shown in Fig. 1a. In the presence of glide plane symmetry this is not allowed and the dominant process becomes the coupling between  $+2k_F$  and  $-2k_F$  phonons. This provides an umklapp scattering channel for the electron-electron interaction as in Fig. 1b. The main point is that this interaction is retarded, depends

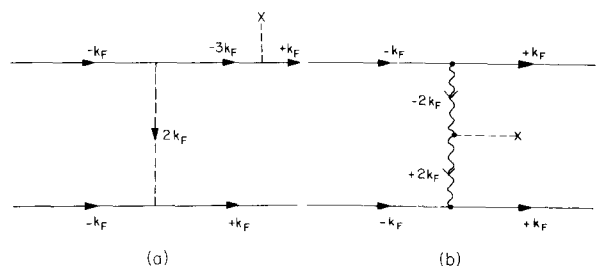


Fig. 1. Umklapp scattering in presence of an external potential of period  $4k_F$ .  
 a) non-retarded process involving electron scattering;  
 b) retarded process via two phonons.

strongly on the phonon frequency and is suppressed by pressure. We shall show that this suppression can result in a crossover from SDW to superconducting ordering.

In our previous work on the competition between the different types of order in quasi-one-dimensional compounds we adopted a model with interchain tunneling represented by the electron dispersion:<sup>7</sup>

$$\epsilon(p) = v_F (|p_x| - p_F) - t_{\perp} (\cos bp_y + \cos cp_z), \quad (1)$$

where  $v_F$  is the Fermi velocity,  $b, c$  are the lat-

tice constants in the transverse directions and  $t_{\perp}$  is the overlap integral which measures the interchain coupling. The interesting range of values of  $t_{\perp}$  is

$$4T_c \lesssim t_{\perp} \lesssim 3 (T_c T_F)^{1/2} \quad (2)$$

where  $T_F$  is the Fermi temperature and  $T_c$  - the mean field Peierls transition temperature for  $t_{\perp}=0$ . The lower limit is determined by the applicability of mean field theory and the upper limit assures sufficient nesting (i.e.  $\epsilon(\vec{q}_0+\vec{p}) = -\epsilon(-\vec{p})$ , for all  $\vec{p}$  ( $p < 0$ ) near the Fermi surface and  $\vec{q}_0 = (2k_F, \pi/b, \pi/c)$  for the possibility of a Peierls transition. In this region the Cooper channel and the Peierls channel are decoupled and the most divergent set of diagrams reduces to that of the Hartree-Fock scheme for each of the possible types of order separately<sup>8</sup>. This scheme was studied previously for non-retarded interactions,<sup>9</sup> and it was shown that the four phases occurring for weak coupling (spin density wave (SDW), charge density wave (CDW), singlet superconductivity (SS) and triplet superconductivity (TS) are separated by the lines  $g_1 = 2g_2 + |g_3|$  and  $g_1 = 0$  ( $g_1, g_2, g_3$  are the backward scattering, forward scattering and umklapp scattering coupling constants, respectively). This phase diagram bears a remarkable similarity to that obtained in the strictly one-dimensional case ( $t_{\perp} = 0$ ) at  $T = 0$ .<sup>10</sup>

Let us now extend the calculation of ref. 9 to include the retarded interactions. This was partly done in ref. 8 where the competition between superconductivity and CDW was discussed in a model based on the Frohlich Hamiltonian with electron-phonon coupling constants  $g_{1p}, g_{2p}$  for  $q \sim 2k_F$  and  $q \sim 0$  phonons, respectively. At present we want to include in the Hamiltonian also the nonretarded electron-electron forward ( $g_{2e}$ ) and backward ( $g_{1e}$ ) interaction, as well as the umklapp scattering mentioned above. Let us define dimensionless coupling constants

$$\begin{aligned} \bar{g}_{ie} &= g_{ie} N(0)/2, \\ \lambda_i &= \frac{2}{g_{ip}} N(0)/\omega_0, \end{aligned} \quad (i = 1, 2) \quad (3)$$

where  $N(0) = 2/\pi v_F$  is the density of states and  $\omega_0$  is the phonon frequency.

The gap equations for the different types of order are obtained in the Hartree-Fock scheme from the lowest order irreducible self-energy diagrams.<sup>9</sup> Retardation effects are due to the phonon interactions in the exchange part of the self-energy. The direct part (Hartree term) which appears in the case of CDW, involves only an  $\omega = 0$  interaction line, and therefore even the phonon lines which contribute to this term are non-retarded. The gap equations are

$$\begin{aligned} \Delta_n &= \frac{1}{2} g^{-N} \int_{-E_c}^{E_c} d\epsilon T \sum_m \frac{\Delta_m}{\epsilon^2 + \epsilon^2 + \Delta_m^2} + \\ &+ \frac{1}{2} g^{-R} \int_{-E_c}^{E_c} d\epsilon T \sum_m \frac{\Delta_m}{\omega_m^2 + \epsilon^2 + \Delta_m^2} \frac{\omega_0^2}{(\omega_n - \omega_m)^2 + \omega_0^2} \end{aligned} \quad (4)$$

where  $\omega_n = 2\pi T n$  are the Matsubara frequencies  $E_c$  is the electron cutoff energy and the compo-

site retarded ( $g^-$ ) and non-retarded ( $g^+$ ) coupling constants are given in table 1, with  $\lambda_3 = 0$ , since we have still not taken into account the umklapp process.

Let us now consider the umklapp process specific to the  $(TMTSF)_2X$  compounds. The acceptor molecule chains produce a static potential along the conducting donor chains of the form

$$W = W_0 \exp(i4k_F R_n) + \text{h.c.}, \quad (5)$$

where  $R_n$  are the coordinates of the donor molecules. Expanding to second order in the molecular displacement we find that this potential adds to the Hamiltonian a term

$$H_u = W_0 (4k_F)^2 \sum_q \frac{1}{M\omega_q} \phi_q \phi_{q+4k_F} + \text{h.c.}, \quad (6)$$

where  $\phi = b + b^+$  ( $b, b^+$  are the phonon destruction and creation operators). The lowest order effect of this term involves the coupling be-

TABLE I

	$g^-$	$g^+$
SS	$-\bar{g}_{1e} - \bar{g}_{2e}$	$\lambda_1 + \lambda_2$
TS	$\bar{g}_{1e} - \bar{g}_{2e}$	$-\lambda_1 + \lambda_2$
CDW	$-2\bar{g}_{1e} + \bar{g}_{2e}$	$-\lambda_2 - \lambda_3$
SDW	$\bar{g}_{2e}$	$-\lambda_2 + \lambda_3$

tween two phonons with momenta  $\pm 2k_F$  and contributes an umklapp term to the electron self-energy. The contribution to the non-retarded direct part of the self-energy affects only the CDW adding  $g^-$  (table 1) the coupling constant  $2\lambda_3$ , where

$$\lambda_3 = |\lambda_1| \frac{2|W_0|4k_F^2}{M\omega_0^2} \quad (7)$$

The exchange term involves an umklapp contribution in the CDW and the SDW channels and adds to eq. (4) a term

$$\pm \lambda_3 \int_{-E_c}^{E_c} d\epsilon T \sum_m \frac{\Delta}{m \omega_m^2 + \epsilon^2 + \Delta_m^2} \left( \frac{\omega_0}{(\omega_n - \omega_m)^2 + \omega_0^2} \right)^2 \quad (8)$$

The two signs in eq. (8) correspond to the two extreme values of the phase of the density waves and are chosen so as to give the highest transition temperature with the reservation that the contributions to the direct and exchange terms have opposite signs. This prescription gives for the CDW a plus sign in the direct term and a minus sign in the exchange term. In the case of SDW there is no direct term and eq. (8) is chosen with a plus sign.

Next, we solve Eq.(4) with the umklapp term (eq. 8) in the weak coupling limit,  $\bar{g}_{ie}, \lambda_i \ll 1$  and  $T \ll \omega_0 \ll E_c$ . In this case the main effect of the phonon propagators in eqs. 4, 8 is to replace the cutoff energy  $E_c$  by  $\omega_0$ . The

umklapp term in eq. 8 may be incorporated into the retarded part of eq. 4 and the latter may be approximated by a simple BCS equation with two cutoffs for the transition temperature to the different types of order

$$1 = \frac{g^R}{2} \int_{-\omega_0}^{\omega_0} d\varepsilon \frac{\tanh(\varepsilon/2T_c)}{2\varepsilon} + \frac{g^N}{2} \int_{-E_c}^{E_c} d\varepsilon \frac{\tanh(\varepsilon/2T_c)}{2\varepsilon} \quad (9)$$

where the coupling constants  $g^N, g^R$  for the different phases are given in table 1. The solution of this equation is

$$T_c = \omega_0 \exp\left\{-\left[\frac{1}{2}g^R + \frac{g^N}{1 - \frac{1}{2}g^N} \ln(E_c/\omega_0)\right]^{-1}\right\} \quad (10)$$

The effect of the different cutoffs for the retarded and non-retarded interactions is to modify the coupling constants for the latter exactly in the same way as the Coulomb interaction parameter  $\mu$  is changed to  $\mu^*$  in the usual expression for the superconducting  $T_c$ .<sup>11</sup>

The accuracy of eq. (10) can be checked by comparing it with the numerical solution of eq.4 for the CDW-SS boundary line, derived in ref. 8 for  $g_{1e} = g_{2e} = \lambda_3 = 0$ . In this case, eq.10 for  $T_{SS} = T_{CDW}$  yields the line

$$\lambda_2 = \frac{\lambda_1}{2} \frac{1 + \lambda_1 \ln(E_c/\omega_0)}{1 - \lambda_1 \ln(E_c/\omega_0)} \quad (11)$$

Comparison with fig. 9 of ref. 8 gives less than 10% deviation for  $\lambda_1 < 0.4, \omega_0/E_c < 0.3$ .

The phase diagram is obtained by comparing  $T_c$  for the four instabilities. The highest  $T_c$  determines the type of order at each point in the interaction-parameter space. The result is shown in Fig. 2, to lowest order in  $g \ln(E_c/\omega_0)$ , in the  $(\bar{g}_1, \bar{g}_2)$ -plane, where  $\bar{g}_1 = g_{1e}^{-\lambda_1}, \bar{g}_2 = g_{2e}^{-\lambda_2}$ . The full lines are the coexistence lines for  $\lambda_3 = 0$ . The dotted lines are the boundary lines of the regions in which SS and SDW may at all occur.  $T_c$  for SS is zero on the line  $\alpha$  and it increases as one moves to the left, while  $T_c = 0$  for SDW on the line  $\beta$  and it increases as one moves to the right. This phase diagram has a new feature compared to the case of non-retarded interactions. The degeneracy of the point at the origin at which all four phases coexist is lifted and one gets two points, A and B, at which three phases coexist. This implies that a SS-SDW co-existence line is now possible (i.e. the line AB in fig. 2).

Including the umklapp scattering, the density wave phases are enhanced resulting in the motion of point B along the TS-SS coexistence line and the motion of point A until at some critical  $\lambda_3 = \lambda_3^*$  both coincide at point P, where

$$\lambda_3^* = [(\lambda_2 + \frac{1}{2}\lambda_1)^2 + 2\lambda_1\lambda_2]^{1/2} - \lambda_2 - \frac{1}{2}\lambda_1 \quad (12)$$

The motion of points A,B is accompanied by a shift of the line  $\beta$  to the left, while the line  $\alpha$  remains intact. For  $\lambda_3 > \lambda_3^*$  a TS-CDW coexistence line appears. This completes the theoretical

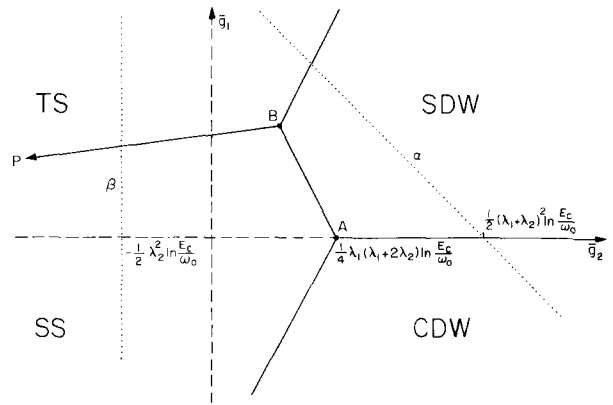


Fig. 2. Phase diagram in the  $(\bar{g}_1, \bar{g}_2)$ -plane. ( $\bar{g}_1 = g_{1e}^{-\lambda_1}, \bar{g}_2 = g_{2e}^{-\lambda_2}$ ). Full lines are the coexistence lines for  $\lambda_3 = 0$ . The dotted lines are the boundary lines of the regions of existence of SS and SDW. The co-ordinates of point A, and of the intersections of the  $\alpha, \beta$ -lines with the  $\bar{g}_2$ -axis are indicated.

analysis of the phase diagram in the presence of retarded and nonretarded interactions and we proceed to a discussion of the experimental data.

We assume that the observed superconductivity in  $(TMTSF)_2X$  compounds is of the singlet pairing type; triplet pairing is unlikely since it is easily suppressed by impurities.<sup>12</sup> Thus, in our picture the change from SDW- to SS- ordering implies the crossing of the AB line from right to left. This seems to happen in several of the  $(TMTSF)_2X$  compounds under pressure. Let us first see if this behaviour can be understood without the umklapp scattering ( $\lambda_3 = 0$ ). We expect that the main effect of pressure is to increase the phonon frequencies and thereby to reduce  $\lambda_1, \lambda_2$ , leaving  $g_{1e}, g_{2e}$  almost unchanged. This means that under pressure a point in the  $(\bar{g}_1, \bar{g}_2)$ -plane on the right-hand-side of the line AB would move away from this line. But even if this were not the case and such a point would move to the left, we would find that  $T_{SDW}$  decreases and  $T_{SS}$  most likely increases (unless AB is crossed upwards at a very small angle). However, experiment shows that both temperatures decrease under pressure. For these reasons we believe that a model with the interactions  $g_{1e}, g_{2e}, \lambda_1, \lambda_2$  alone is unlikely to explain the observed behaviour.

Let us now consider the effect of the umklapp scattering parameter  $\lambda_3$ . First note that from eqs. (2), (7) it follows that  $\lambda_{3\omega} \sim \omega^{-4}$  (from (7) and  $\lambda_{1\omega} \sim \omega^{-2}$ , since  $\lambda_1 = (J^2 n(\epsilon_F) / M \omega^2)^0$ , where  $J$  is an electronic matrix element). Therefore, this interaction is the most sensitive to pressure. When the pressure is reduced,  $\lambda_3$  increases and line AB moves to the left. This behaviour explains the experimental results quite naturally. In this picture the transition from SDW to SS-ordering is due mainly to the shift under pressure of the AB line to the right, rather than to the change of position in the  $(\bar{g}_1, \bar{g}_2)$ -plane. Since  $\lambda_3$  appears in the exponent

of  $T_{SDW}$  and not of  $T_{SS}$ , while  $\lambda_1$  appears in the exponent of  $T_{SS}$  and not of  $T_{SDW}$ ; and both coupling constants decrease under pressure<sup>13</sup>, the crossover from the SDW to the SS-phase occurs with  $T_{SDW}$  and  $T_{SS}$  decreasing with pressure. Since  $\lambda_3$  is more sensitive to pressure (e.g.  $d\ln\lambda_3/d\ln a \sim -10$ ,  $\lambda_3 \propto \omega^{-2}$ ,  $\lambda_3 \propto \omega^{-4}$ ,  $(d\ln\lambda_1/d\ln a) \sim 20$ ,  $(d\ln\lambda_2/d\ln a) \sim 40$ , where  $a$  is the lattice constant along the chain), we expect a stronger pressure dependence of  $T_{SDW}$  than of  $T_{SS}$ , which is again consistent with experiment:  $dT_{SS}/dP = 0.087 \text{ K/kbar}$ <sup>14,17</sup>;  $dT_{SDW}/dP = 1-2 \text{ K/kbar}$ .<sup>2</sup>

We wish to point out that the glide plane symmetry of the acceptor chains plays a key role. If not for this symmetry, we would have a gap in the electron spectrum at  $\pm 2k_F$ , which would result in a half-filled band and consequently a non-retarded electron-electron umklapp scattering  $g_{2e}$ . The lowest order of such a process when allowed by symmetry is shown in Fig. 1a. Its coupling is  $\alpha g_1 e^W/E_F$ , which can be of the order of magnitude of  $\lambda_3$ .

It was recently found<sup>6</sup> that  $(TMTSF)_2ClO_4$  is superconducting at ambient pressure below  $1.3 \text{ K}$ . The  $ClO_4$  ions appear to be disordered<sup>6</sup> in this compound. A possible explanation in the line of the present model of the superconductivity in this case, is that the disorder excludes the possibility of umklapp scattering and pressure is not necessary to suppress  $\lambda_3$  in order to recover the favorable conditions for superconductivity. Another explanation is that the disorder of the acceptor chains acts as impurity scattering for electrons, which suppresses the spin-density waves, but has only a small effect on singlet superconductivity.<sup>12</sup> Note that in HMTSF-TCNQ, lattice disorder destroys the Peierls state and gives rise to a metallic state at  $0 \text{ K}$ <sup>15</sup>.

Another possible explanation to the pressure effect in these compounds is that pressure increases the interchain coupling and thereby destroys the nesting of the Fermi surface. This effect was evaluated for Eq.(1) when the linear dispersion in the x-direction was replaced by a nonlinear one, e.g. a free electron dispersion.<sup>7</sup> The result shows that the CDW transition (and similarly for SDW) is suppressed when  $t_{\perp} > 3(T_{CF})^2$  (eq.(2)). In this case superconductivity may appear<sup>16</sup>. For  $(TMTSF)_2PF_6$ ,  $T_C \approx 2000 \text{ K}$ ,  $T_C \approx 18 \text{ K}$  and the above condition is  $t_{\perp} > 600 \text{ K}$ . This number seems to be rather high, especially judging by the large anisotropy of the electric conductivity at ambient pressure. This anisotropy seems to be reduced strongly by pressure<sup>17</sup>, reaching a value of  $\sigma_b(4.2 \text{ K})/\sigma(4.2 \text{ K}) \approx 7$  at  $10 \text{ kbar}$ . However, there is experimental evidence that in spite of that, the nesting property of the Fermi surface is not destroyed by pressure. The authors of ref. 17 find a gap over most of the Fermi surface, indicating the formation of density waves. The "one-dimensional" picture used here does not depend on the value of  $t_{\perp}$ , as long as the nesting property is preserved.<sup>7</sup>

Recently, Kwak et al<sup>18</sup> observed Shubnikov-deHaas oscillations at  $7.5 \text{ kbars}$  in  $(TMTSF)_2PF_6$ , indicating electron and hole pockets of equal cross-sectional areas of less than 1% of the Brillouin Zone, and an effective mass close to  $m_0$ . Such pockets were observed and accounted for<sup>19</sup> in the two-chain compound HMTSF-TCNQ. They were also observed below the Peierls transition in the one-chain system  $NbSe_3$  by transport methods.<sup>20</sup> Such pockets are expected in general in a two-chain system due to the deviations from a planar Fermi surface<sup>19</sup>, and in monochain systems whenever there are deviations from perfect nesting of the Fermi surface, and the nesting vector  $q_0$  becomes a reciprocal lattice vector (in presence of CDW's or SDW's). In the latter case the two sheets of the Fermi surface are almost equivalent, and shifting one of them by the nesting vector results in small electron and hole pockets. It is reasonable to assume that in  $(TMTSF)_2PF_6$ ,  $\vec{q}_0 = (2k_F, \pi/b, q_c)$  (the value of  $q_c$  is less certain but irrelevant for the present argument), and that this vector at  $P = 7.5 \text{ kbars}$  is still a reciprocal lattice vector due to the presence of SDW's<sup>17</sup>. This results in small banana-shape electron and hole pockets with a volume of the order of  $(t_{\perp}/t_{\parallel})^2$  of the Brillouin zone. This explains why the significant decrease in the resistance anisotropy and the appearance of Shubnikov-deHaas oscillations at high pressure are consistent with each other, and with the suggestion that the deviation from perfect nesting is small. This point will be discussed in greater detail elsewhere.

Eq. (5) implies an isotope shift parameter  $\alpha = -\frac{1}{2} d\ln T_C/d\ln \omega_0$  ( $g^N, g^R$  are independent of the ion mass  $M \propto \omega_0^{-2}$ ) which gives

$$\alpha = \frac{\frac{1}{2}(g^N)^2}{(g^N + g^R - \frac{1}{2}g^R \ln \frac{E_C}{\omega_0})^2}^{-\frac{1}{2}} \quad (13)$$

If the couplings  $g^N, g^R$  cancel each other to a large extent so that  $T_C$  is very low,  $\alpha$  can be very large. Numerical solutions of Eq. (4) for the CDW problem<sup>21</sup> have shown that  $\alpha$  is reasonably large and positive ( $\alpha \approx \frac{1}{2}$ ) even without such cancellation if  $\omega_0 \geq 2\pi T_C$ . Subsequent measurement on TTF-TCNQ<sup>22</sup> have indeed observed a positive isotope shift in this CDW system.

The model presented in this paper is an additional example of the possibility to affect the competition between insulating and superconducting phases in quasi-one-dimensional conductors by applying pressure. This was first suggested by us in the context of the competition between CDW's and superconductivity<sup>23</sup>. What is new here is that the insulating phase may be a SDW and the special role of the umklapp process.

#### References

1. K. Bechgaard, C.S. Jacobsen, K. Mortensen, H.J. Pedersen and N. Thorup, Solid State Communications, **33**, 1119 (1980).
2. D. Jerome, A. Mazaud, M. Ribault and K. Bechgaard, Journal de Physique Lettres **41**, L95 (1980);  $T_C \approx 1.2 \text{ K}$  at  $6.5 \text{ kbars}$  was reported in refs. C14 and 17.
3. H.J. Pedersen, J.C. Scott and K. Bechgaard,

4. Solid State Communications 35, 207 (1980).
5. A. Andriex, D. Jerome and K. Bechgaard, Journal de Physique Lettres 42, L-87 (1981).
6. M. Ribault, J.P. Pouget, D. Jerome and K. Bechgaard, Journal de Physique Lettres 41, L607 (1981); K. Bechgaard et al., preprint
7. K. Bechgaard, K. Carneiro, M. Olsen, F.B. Rasmussen and C.S. Jacobsen, preprint.
8. B. Horovitz, H. Gutfreund and M. Weger, Physical Review, B12, 3174 (1975).
9. B. Horovitz, Physical Review B16, 3943 3943 (1977).
10. B. Horovitz, Solid State Communications 18, 445 (1976).
11. For a review see J. Solyom, Journal of Low Temperature Physics, 1980.
12. P. Morel and P.W. Anderson, Physical Review 125, 1263 (1962)
13. R. Balian and N.R. Werthamer, Physical Review 131, 1553 (1963); H. Gutfreund and W.A. Little, in "Felix Bloch and Twentieth Century Physics", p. 1, ed. M. Chodorow et al., Rice University Studies, 1980.
14. H. Gutfreund, M. Weger and M. Kaveh, Solid State Communications 27, 53 (1978).
15. K. Andres, F. Wudl, D.B. McWhan, G.A. Thomas, D. Nalewajek and A.L. Stevens, Physical Review Letters 45, 1449 (1980).
16. L. Zuppiroli, J. Arionceau, M. Weger, K. Bechgaard and C. Weyl, Journal de Physique Lettres 39, L-170 (1978)
17. B. Horovitz and A. Birnboim, Solid State Communications 19, 91 (1976)
18. R.L. Greene and E.M. Engler, Physical Review Letters 45, 1587 (1980).
19. J.F. Kwak, J.E. Schirber, R.L. Greene and E.M. Engler, preprint.
20. M. Weger, Solid State Communications 19, 1149 (1976).
21. N.P. Ong, Physical Review B 18, 5272 (1978).
22. B. Horovitz, Solid State Communications 19, 1001 (1976).
23. J.R. Cooper, J. Lukatela, M. Miljak, J.M. Febré, L. Giral and E. Aharon-Shalom, Solid State Communications 25, 949 (1978).
24. H. Gutfreund, B. Horovitz and M. Weger, Journal of Physics C7, 383 (1974).